Photodiagnosis and Photodynamic Therapy 25 (2019) 43–49

Contents lists available at ScienceDirect

Photodiagnosis and Photodynamic Therapy

journal homepage: www.elsevier.com/locate/pdpdt

Hypericin-glucamine antimicrobial photodynamic therapy in the progression of experimentally induced periodontal disease in rats

Paula Delello Macedo[a], Sâmara Tfaile Corbi[a], Guilherme José Pimentel Lopes de Oliveira[b], Janice Rodrigues Perussi[c], Anderson Orzari Ribeiro[d], Rosemary Adriana Chierici Marcantonio[a,*]

[a] São Paulo State University (Unesp), School of Dentistry Araraquara, Department of Diagnosis and Surgery, Araraquara, Brazil
[b] Federal University of Uberlândia, Dental School, Department of Periodontology, Uberlândia, MG, Brazil
[c] USP, São Paulo University, Chemistry and Molecular Physics Department, São Carlos, SP, Brazil
[d] UFABC, Federal University of ABC, Centre for Natural Sciences and Humanities, Santo André, SP, Brazil

ARTICLE INFO

Keywords:
Hypericum
Phototherapy
Periodontitis

ABSTRACT

Objective: To evaluate the effect of antimicrobial photodynamic therapy (aPDT) using the photosensitizer hypericin-glucamine in the progression of experimentally induced periodontal disease (PD) in rats.
Material and methods: Subgingival ligatures were inserted around the upper second molars of 30 rats. After 7 days (Baseline), the animals were randomly distributed into 3 experimental (n = 5) groups: Hypericin-glucamine; LED (amber LED, 700 mA, 590 nm, 90 mW, 34.10 J/cm^2); and aPDT (Hypericin-glucamine + LED). The treated hemimaxillae were randomly chosen. The periodontal disease progression was monitored without treatment interference in the opposite hemimaxillaes, which were used as the negative control of each animal. The euthanasia was programmed according to each experimental period, 7 or 15 days after the Baseline. Microtomographic, histometric and Tartrate Resistant Acid Phosphatase (TRAP) immunohistochemistry analyses were carried out.
Results: Computerized microtomography analyses indicated that the aPDT group had a significantly higher percentage of bone tissue when compared to the other 7 days experimental groups. This result was corroborated by the histometric evaluations of the furcal area. The LED-treated group presented the highest percentages of bone volume for the 15 days experimental groups, which is remarkably higher than the groups treated with Hy-g and aPDT. The histometric analyses demonstrated the control groups had greater bone loss in the proximal regions when compared to the treated groups. The aPDT led to a lower osteoclast activity at both 7 and 15 days. Thus, we can conclude that aPDT exhibits positive effects in PD treatment by promoting favorable conditions for periodontal repair.

1. Introduction

Antimicrobial Photodynamic Therapy (aPDT) has been an outstanding subject of scientific study in periodontics. Despite the fact that the number of scientific publications in this topic has been increasing recently, there is an imminent need for new studies that aim at understanding the aPDT mechanisms of action during the periodontal disease development. Two parameters that influence the aPDT effectiveness is the chosen photosensitizer (PS) and the light source. Both should be discussed widely in order to deepening the comprehension of aPDT mode of action and for standardizing the technique to obtain actual benefits in clinical practice.

The aPDT action occurs through the interaction among the light, PS, and local characteristics of the undertreating site. The success of the treatment will depend on light intensity, exposure time, mode of operation and light source wavelength. Laser and light emitting diodes (LEDs) has been the most applied source of light for aPDT [1].

The physical-chemical characteristics of microorganism-PS interaction, such as tissue color, bleeding or fluids, thermal conductivity and pH, and other local factors are another aspects to be considered [1–3]. Moreover, the PS type, concentration and mode of action are issues to be contemplated. That includes the PS relative solubility in water and lipids, ionization constant, certain specific factors, such as light absorption characteristics, and the formation efficiency of a triplet excited

* Corresponding author at: Universidade Estadual Paulista "Júlio de Mesquita Filho" (Unesp), Faculdade de Odontologia, Departamento de Diagnóstico e Cirurgia, Rua Humaitá, 1680, CEP 14801-903, Araraquara, SP, Brazil.
E-mail addresses: paula_mac2@yahoo.com.br (P.D. Macedo), sa_tfaile@yahoo.com.br (S.T. Corbi), guioliveiraodonto@hotmail.com (G.J.P.L. de Oliveira), janice@iqsc.usp.br (J.R. Perussi), anderson.ribeiro@ufabc.edu.br (A.O. Ribeiro), adriana.marcantonio@unesp.br (R.A.C. Marcantonio).

https://doi.org/10.1016/j.pdpdt.2018.11.003
Received 27 July 2018; Received in revised form 21 October 2018; Accepted 2 November 2018
Available online 03 November 2018
1572-1000/

state or singlet oxygen production [1,4].

In view for greater efficiency of microorganism inactivation, modifying the PS hydrophobicity and charge, according to the cellular characteristics of each microorganism, is an effective strategy to overcome some of the current aPDT challenges [5–8].

Hypericin (Hy-g) has several interesting properties for use as a photosensitizer for aPDT [9]. However adequate solubility in water is crucial to the process, and this compound is barely soluble in aqueous solutions [10]. An effective way to improve its solubility is obtaining a mix the laboratory. In this study, we used the hypericin-glucamine (Hy-g) sinthetyzed from mixing the hypericin and the N-methylglucamine in water, obtaining the Hypericin-glucamine.

Hypericin-glucamine (Hy-g) exhibits several desirable properties as a PS for aPDT, which includes a high quantum yield of singlet oxygen generation, high extinction coefficient close to 600 nm and relatively low dark toxicity [11,12]. Studies have demonstrated significant phototoxic hypericin power in PDT treatment of psoriasis and other skin diseases [13,14]. It also has powerful anti-cancer activity, since it induces both apoptosis and tumor cell necrosis [15], and the ability to promote microorganism inactivation [12,15–18]. Some studies considered it one of the most potent PS found in nature [19–21]. In this context, the present study aims at evaluating the action of Hypericine-glucamine aPDT activated by an amber LED (34.10 J/cm^2) source in the progression and development of experimentally induced periodontal disease (PD) in rats.

2. Material and methods

2.1. Animals

Thirty male adult rats (*Rattus norvegicus albinus*), weighing between 300–330 grams were subjected to this analysis. The animals were kept in plastic boxes with a maximum of three animals per box, in a controlled light, humidity and temperature environment. The study was submitted to the Ethics Committee on Animal Use (CEUA n ° 07/2012).

2.2. The Hypericin-glucamine preparation and standards

The hypericin-glucamine used as PS was synthesized by Prof. Dr. Anderson O. Ribeiro (Federal University of ABC, Brazil). From his working solution, a stock solution of 200 μmol.L^{-1} was made in a polar aprotic solvent – dimethyl sulfoxide (DMSO) – and sterilized by filtrating the solution using a 0.22 μm membrane. To enhance the PS action, an ointment was prepared by diluting the stock solution in sodium phosphate buffer (pH 7.2), which resulted in a semi-solid substance with final concentration of 10 μg mL^{-1} and DMSO percentage less than 1%. The ointment was obtained 15 days before its usage at the Photosensitizer Laboratory from the São Carlos Institute of Chemistry, University of São Paulo (IQSC-USP, Brazil). All procedure was carried out in dark environment to prevent any pre-treatment activation.

2.3. Periodontal disease induction

The animals were anesthetized with a combination of Xanthine (Virilaxine Hydrochloride - Virbaxyl 2% - Virbac do Brasil Ind. e Com. Ltda.) and Ketamine (Ketamine Hydrochloride - Francotar 3% - Virbac do Brasil Ind. And Com.), at 0.08 mL/100 g and 0.04 mL/100 g body weight, respectively. Cotton strands (n^o 24, Cotton Chain, Coats Corrente Ltda., São Paulo, SP, Brazil) were inserted into the subgingival region around both upper second molars for PD induction and maintained throughout the experimental period until animal euthanasia.

2.4. Experimental groups

All treatments for each experimental group were carried out after 7 days of ligature insertion (Baseline). The treated hemimaxilla (right or left) was chosen randomly and its contralateral hemimaxil was used as negative control. The animals were randomly distributed among groups (n = 5):

- **Hy-g (Hypericin-glucamine) Group:** 1 mL (approximately, 0.2 mg of PS ointment) was deposited in the groove, maintained in the dark for 10 min (incubation time), and removed with the aid of a cotton swab;
- **LED Group:** An amber-colored LED (tip diameter of 11 mm, wavelength of 590 nm, 700 mA, and converted power of 90 Mw) was developed by MM Optics (São Carlo/SP – Brazil). The specific wavelength matches to the equivalent maximum absorption band for the hypericin but does not alter for hypericin-glucamine. The diameter of the tip was adequate to simultaneously cover all under-treating tooth faces. Thus, a transmucosal LED application was performed for 6 min, which resulted in a 34.10 J/cm2 dosage.
- **aPDT Group (Hy-g + LED):** the PS was applied as described for the Hy-g group followed by LED activation as described for the LED group.

Animals were euthanized 7 or 15 days after the baseline with anesthetic overdose. Then, the hemimaxillae were removed and fixed in paraformaldehyde (4%, cured period of 48 h). Following this, each sample was washed in running water for 24 h and stored in 70% alcohol.

3. Digital microtomography evaluation (μCT)

Samples were submitted to X-ray beam scanning in a computerized digital microtomography system, which evaluates the percentage of bone volume present in the upper second molar region in view to quantify the bone tissue. All parts were scanned using a SkyScan microtograph (SkyScan 1176 Bruker MicroCT, Aatselaar, Belgium, 2003),using an Al 0.5 mm filter, voxel size of 17.48 μm, 50 KV of voltage, and 500 mA of electric current. The resulting images were stored and, then, reconstituted by the NRecon software. They were rotated and repositioned in a standard orientation using the DataViewer software and, then, saved in the coronal plane. Finally, the CTAnalyser software was used to define the region of interest (ROI) [22,23]. Two ROIs were defined. The first one comprised the second molar in the coronoid/apical sense of the furcation ceiling region up to 1,000 μm in the apical direction until its proximal limitations with neighboring teeth. The second one was selected from the same anatomical delimitation of the first ROI, but circling and covering only the roots of the second molar. To obtain the percentage of bone volume, the second ROI was subtracted from the first one.

4. Histological processing

After the computerized microtomography analysis, the hemimaxillae were washed again in running water for 24 h and submitted to a decalcification process. A histological processing routine was conducted by embedding the hemimaxillae in paraffin in the mesio-distal direction along the axis of the tooth. Cuts of four micrometers were made and three cuts were place in histological slides. A total of 10 slides were obtained for each hemimaxilla. Slides 1, 3, 4, 5 and 7 were stained by using the hematoxylin-eosin (HE) technique and then submitted to the histometric analyses; while slides 2, 6 and 10 were reserved for the immunohistochemical analyses.

5. Histometric analyses

5.1. Furca and proximal area

Images from the second molar were captured and saved in a local computer using a DIASTAR optical microscope (Leica Reichert & Jung

products, Germany), under X40 magnification, with support of a DXC-1107 A/107 A P video camera (Sony Electronics Inc, Japan).

Three histological images, which corresponded to the initial, middle and final part of the sample from each animal, were measured using the Image J – Launcher software (version 1.48b, National Institutes of Health, USA). The investigated area was defined by measuring 1000 μm in the apical direction from the furcation top region and limited horizontally by the roots of the second molar [24,25]. To evaluate the bone loss extension in the proximal area, photomicrographs (magnification, x10) were used. Horizontal lines were drawn from the cement-enamel junction until the bone crest height. A trained blind examiner conducted all described measurements.

6. Immunohistochemical assessment

The immunohistochemistry was performed to understand the distribution and localization of expressed tartrate-resistant acid phosphatase (TRAP) protein. Non-specific epitopes were blocked by applying a 3% hydrogen peroxide for 30 min and 3% bovine albumin protein (BSA) for 2 h. Then, the samples were incubated for 16 h in primary antibody (1:100 ration, Abcam, Inc. Cambridge, MA, USA).

Some slides were subjected to IgG (R&D Systems, Minneapolis, MN, USA) treatment instead of the primary antibody at the same solution as negative controls. Subsequently, these cuts were treated by avidin-biotin-peroxidase (ABC) complex method using the ABC Staining System kit (ABC kit DAKO A/S, Copenhagen, Denmark), following the manufacturer's instructions. These slides were counterstained on Carrazi hematoxulin solution for visualizing the cell nuclei.

The TRAP analysis was carried out by counting the stained osteoclasts in contact with the bone tissue in the furcation region and around the second molar [25]. The sum of the osteoclast values present in both regions of interest was calculated. All analyses were performed by a blind and trained examiner.

7. Statistical analyses

The experimental data were statistically evaluated using the Shapiro-Wilk normality test while data concerning the analyses between the treated hemimaxillae and their negative controls were submitted to the paired Student's t-test. Comparisons among the treated groups were carried out by the Anova parametric test complemented by the Tukey test. The power of the study was at least 95% for a 5-animal sample ($p < 0.05$) and Graphpad 5.0 software (Graphpad Prism version 5.00 for Windows, GraphPad Software, La Jolla California, USA) supported all statistical analyses (Fig. 1).

8. Results

8.1. Computerized microtomography (MCT)

The X-ray micrograph analysis assessed the percentage of bone tissue present in the second molar region. No significant difference was observed between the treated hemimaxillae and the control side for both experimental periods, although treated groups exhibited a trend of higher percentage of bone tissue volume (Graph 1). Hemimaxillae treated with aPDT showed a significantly higher percentage of bone tissue volume than those treated only with Hypericin-glucamine only in the 7 days experiment ($p < 0.01$).

8.2. Histometric analyses

8.2.1. Furca region

To the 7 days experimental group, the hemimaxillae treated with hypericin-glucamine ($p < 0.01$) and LED ($p < 0.001$) exhibited greater bone volume percentages in the furcation region compared to the control side. Higher bone volume percentage in the treated hemimaxillae was also observed in all groups. It is also notable that the hypericin-glucamine treated hemimaxillae from the 7 days experimental group showed higher bone volume percentage when compared to LED-treated hemimaxillae ($p < 0.05$). Furthermore, those hemimaxillae treated with aPDT also exhibited greater value of bone tissue percentage than those treated only with hypericin-glucamine ($p < 0.01$) or LED ($p < 0.001$) (Graph inlay in Fig. 2).

To the 15 days experimental group, the LED-treated group presented the highest bone volume percentage, even when compared to the groups treated with hypericin-glucamine ($p < 0.001$) and aPDT ($p < 0.05$) (Graph inlay in Fig. 2)

8.2.2. Interproximal region

All control groups had noteworthy bone tissue loss when compared to the treated ones (Graph 1). Regarding the 7 days treated groups, the LED one exhibited significantly higher interproximal bone loss than the aPDT (< 0.01) and Hypericin-glucamine ($p < 0.001$) groups. Moreover, the aPDT group also lost more bone volume than the group treated only with Hypericin-glucamine ($p < 0.01$). No significant differences were detected between the proposed 15 days treated groups (Fig. 3).

8.3. Immunohistochemistry assessment

The control groups manifested the highest TRAP staining and trend for greater staining values the longer the period of presence of ligature (Graph 2). Significantly fewer positive TRAP cells for the aPDT group were observed within days after treatment when compared to the controls groups all periods analysed. After 15 days, lower staining was observed to aPDT ($p < 0.01$) and LEDs ($p < 0.01$) groups in relation to the control group.

9. Discussion

The effects of aPDT and its components, Hy-g and an amber LED source, were assessed concerning PD progression and development. When the isolated effect of Hypericin-glucamine was evaluated 7 days after treatment, a significantly higher bone tissue percentage in the furcation area was detected as well as less bone loss in the interproximal region when compared to the control groups that received no treatment. These results were better explained by the immunohistochemical analyses, which indicates a lower osteoclast cell staining in the Hy-g treated hemimaxillae compared to the control groups. The results are corroborates the literature, which reports that Hypericin effects as a drug – not as a PS – and that it presents therapeutic action with anti-inflammatory and biomodulating properties [26–28].

Previous studies [10,12,29] verified the best conditions for the photoinactivation of *S. aureus* and *E. coli*, testing hypericin and its hydrophilic derivative, hypericin-glucamine, activated by an amber LED, similar to the present study. Due to Hy-g hydrophilicity, the authors could conclude that greater intracellular PS accumulation in the microorganisms was possible without harming their selectivity, though. In this study, we observed the lowest bone loss occurred in the aPDT-treated group while the highest bone tissue percentage was detected by digital microtomography for the 7 days period of treatment - also in the aPDT-treated group. This can be explained as consequence of the osteoclast activity, which showed a significant lower value for this experimental group in both experimental periods.

Light wavelength, intensity, time of exposure and operational mode of the light source are aspects to be considered in the photodynamic therapy. [1]. An amber colored LED was applied herein and, after 7 days, lower osteoclastic activation was observed, leading to higher bone tissue percentages in the furcation region and lower bone loss in the interproximal regions compared to the control hemimaxillae. Other studies corroborate these findings and this evidence the biomodulation

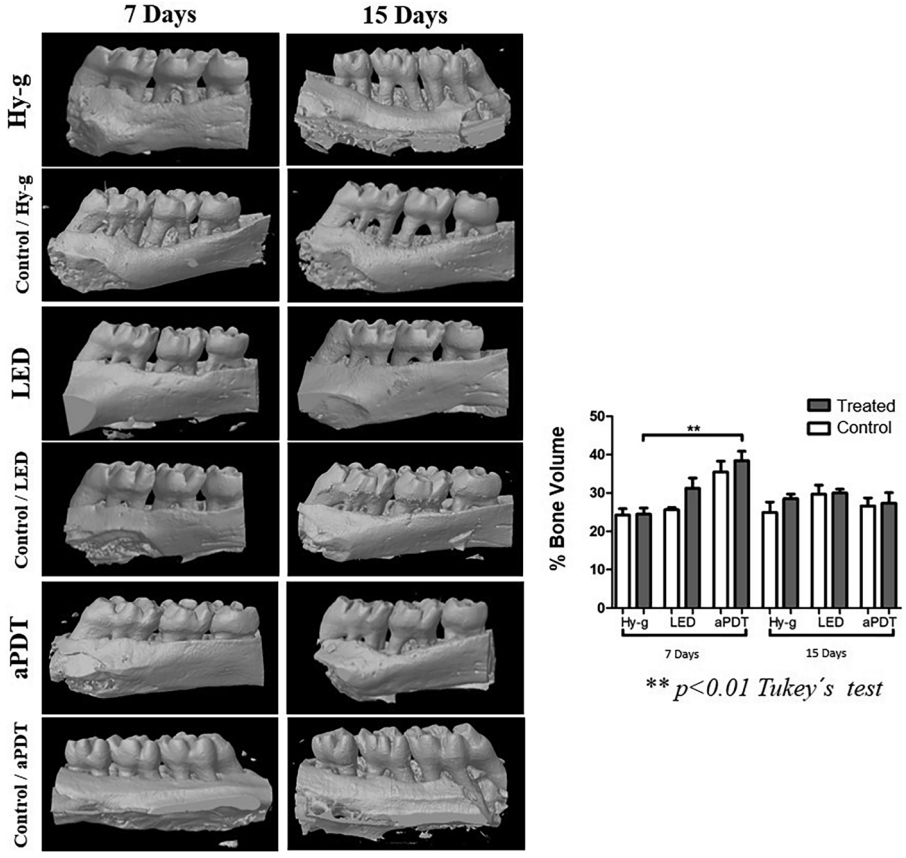

Fig. 1. Panel of the representative 3D images, generated by computerized microtomography. The representation of the bone tissue percentage present in the region of interest (proximal and furcation) of the second upper molar is displayed for the experimental groups and periods.

role of LED sources in periodontal tissue. For instance, Choi et al. [30] analysed the effects of LED application (wavelength of 635 nm) on human gingival fibroblasts treated with *Porphyromonas gingivalis* lipopolysaccharides (LPS) and, comparing to no treat gingival, observed inhibition of proinflammatory cytokine activation. Their result demonstrated that LED irradiation may be clinically useful as anti-inflammatory action. Fonseca et al. [31] analyzed the effects of a LED source application (wavelength of 940 nm) on periodontal healing after experimental orthodontic traction in rats. They reported less osteoclasts and inflammatory cells, as well as increased blood vessels, which suggests a decrease in inflammation and root resorption.

No significant differences between the bone tissue volumetric percentages were observed in the treated groups and their respective control one for the 15 days of experiment in furcation area in both histometric and computerized microtomography evaluations. This result provides a comprehensive reading of the entire second molar region. Although it was necessary for the aims of this study, the continuous induction was sufficient to recolonizing of the sites and remark development of PD. Nonetheless, the model used herein simulates the disease process in areas that are challenging to be accessed in mechanical treatment [25,32,33].

The study individualizing the aPDT components demonstrated that the employed LED and PS did not cause damage to periodontal tissues. Contrariwise, they brought benefits to the treatment of periodontitis, by

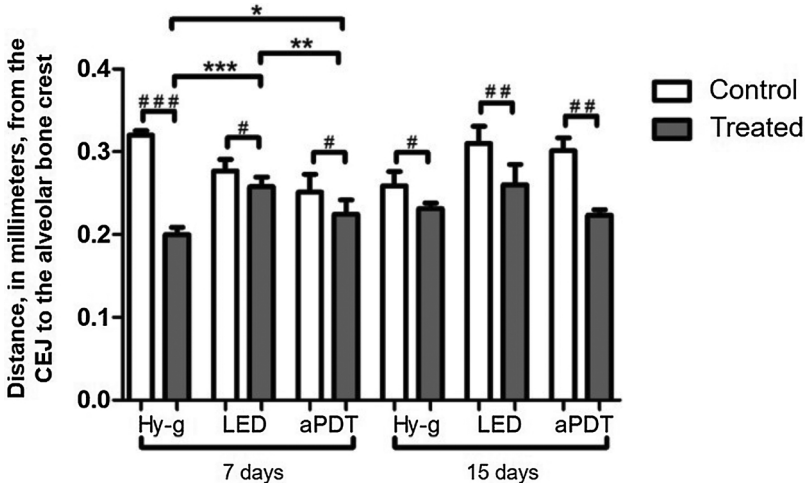

Graph 1. Mean distance (in millimeters) between the cementum enamel junction (CEJ) to the alveolar bone crest located the interproximal region of the upper second molar.
# p < 0.05 Student's *t*-test / ## p < 0.01 Student's *t*-test / ### p < 0.001 Student's *t*-test.
** p < 0.05 Tukey test / ** p < 0.01 Tukey test / ** p < 0.001 Tukey test.*

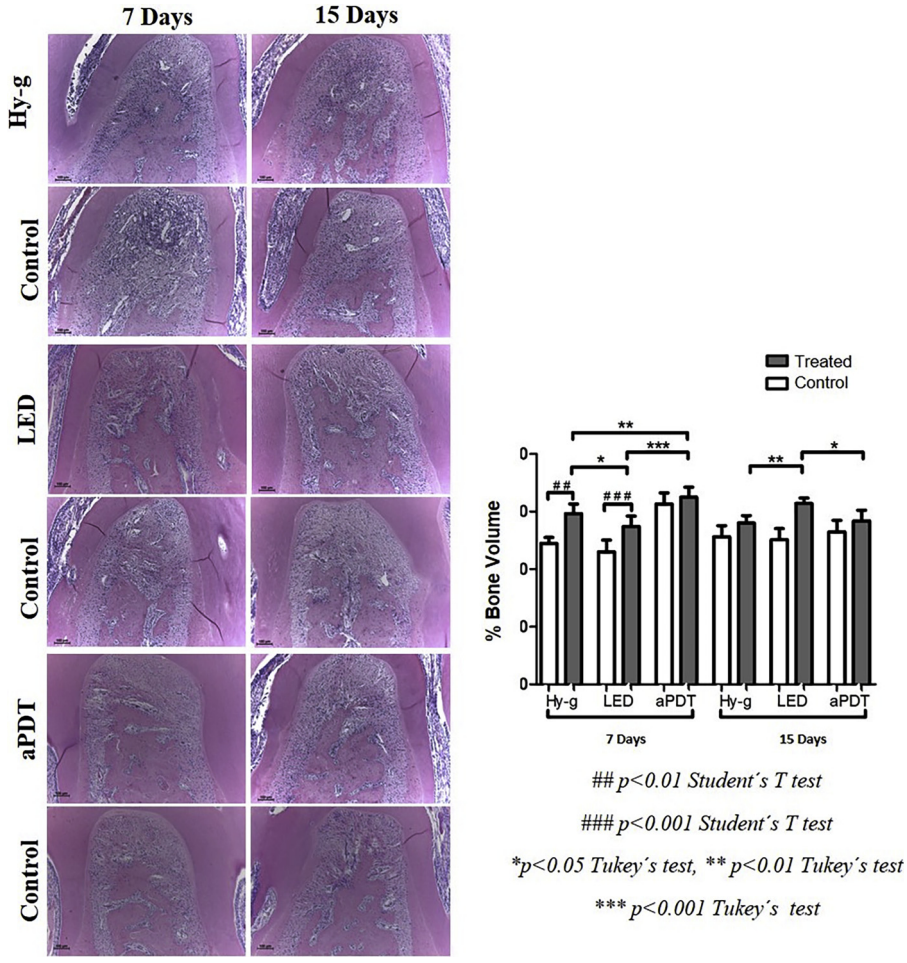

Fig. 2. Photomicrograph panel of the furcation region of all experimental groups, and their respective controls, for the 7- and 15-days experimental periods (HE, 100x). The attached-graphic indicates the mean percentages and standard deviations of bone tissue present in the furcation region of the upper second molar, referring to the different groups and experimental periods evaluated by histometry.

providing a more expressive results when combined in aPDT group. Nevertheless, the understanding of the mechanisms of action of both the LED source and hypericin-glucamine is still a matter of further investigation in view to enhance the technique standards in the periodontal site and to produce more expressive results in clinical usage. he study individualizing the aPDT components demonstrated that the employed LED and PS did not cause damage to periodontal tissues. Contrariwise, they brought benefits to the treatment of periodontitis, by providing a more expressive results when combined in aPDT group. Nevertheless, the understanding of the mechanisms of action of both the LED source and hypericin-glucamine is still a matter of further investigation in view to enhance the technique standards in the periodontal site and to produce more expressive results in clinical usage.

10. Conclusions

The purpose of the current study was to evaluate the action of Hypericine-glucamine aPDT activated by an amber LED source (wavelength of 590 nm, 34.10 J/cm^2 dosage) in the progression and development of experimentally induced periodontal disease in rats. Both hypericin-glucamine and LED exhibited therapeutic properties and contributed to periodontal tissue biomodulation. The outcomes suggest that the aPDT technique, when applied as proposed in this study, is promising. However, we recommend further studies to evaluate the effectiveness of more than one therapy application session and the investigation of the mode of action.

Support

This work received financial support from the Coordination for the Improvement of Higher Level Personnel (BR) - (AUX PG 655/2014), the National Council for Scientific and Technological Development (BR) - (133436 / 2012-8) and FAPESP - São Paulo Research Foundation (2016 / 00275-8).

Ethical approval

Ethical approval was granted by the Araraquara Faculty of Dentistry Ethics Committee on Animal Use (UNESP, Brazil CEUA/FOAr 07/2012).

Conflicts of interest

The authors declare no conflicts of interest.

Acknowledgments

The authors would like to thank technicians Leandro Alves dos Santos and Ana Claudia Gregolin Costa Miranda for their support in the laboratory phases of this study. This study was funded by the Coordination of Personal Improvement of Higher Education (CAPES, Brasilia, DF, Brazil), by the National Council for Scientific and Technological Development (CNPq, Brasília, DF, Brazil) and FAPESP (2016/00275-8).

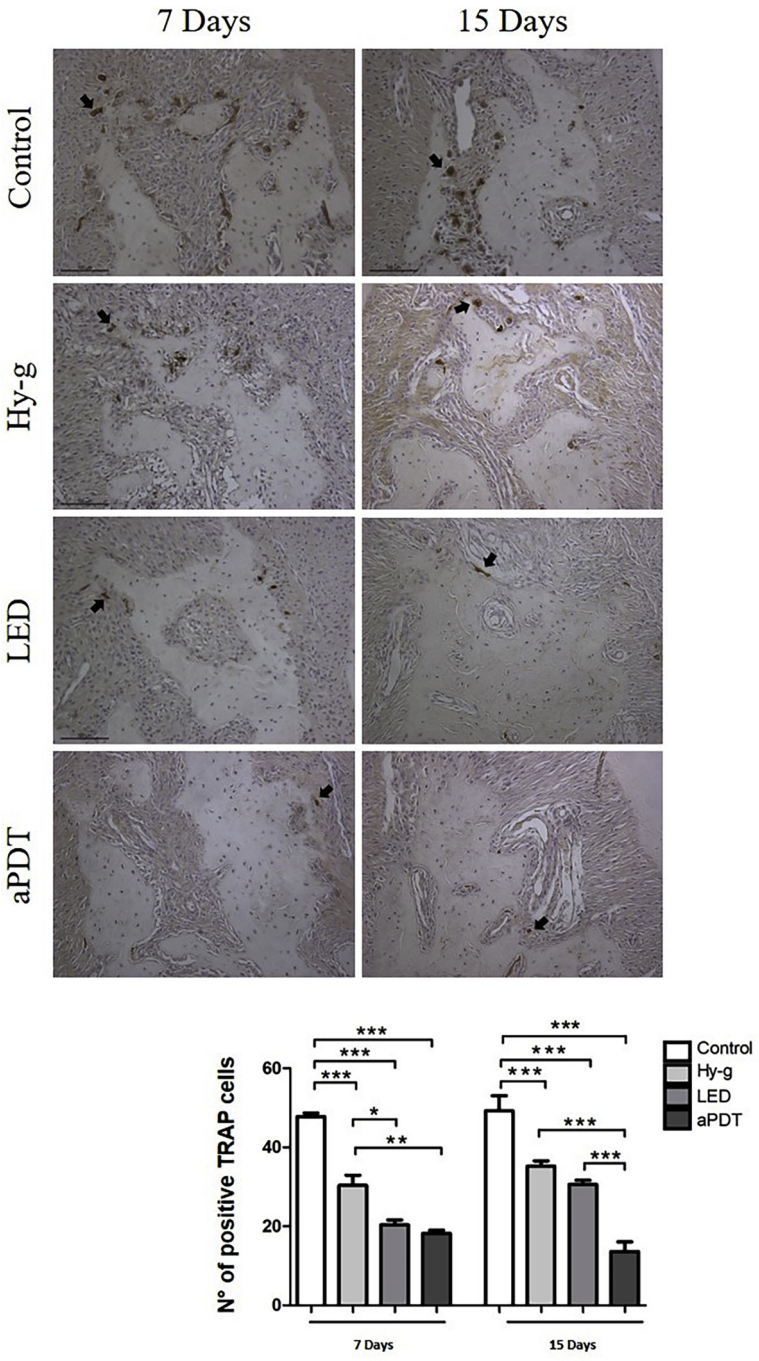

Fig. 3. Representative photomicrograph panel of the immunohistochemical analyses (HE X 100). The arrows point to positively labeled TRAP cells. The attached graph indicates the mean percentages and standard deviations of the number of cells positively labeled for TRAP in the upper second molar region, referring to the different experimental groups and their respective controls, at 7 and 15 days.

References

[1] C.M. Cassidy, M.M. Tunney, P.A. McCarron, R.F. Donnelly, Drug delivery strategies for photodynamic antimicrobial chemotherapy: from benchtop to clinical practice, J. Photochem. Photobiol. B Biol. 95 (2009) 71–80, https://doi.org/10.1016/j.jphotobiol.2009.01.005.

[2] W.C.M.A. Melo, P. Avci, M.N. de Oliveira, A. Gupta, D. Vecchio, M. Sadasivam, R. Chandran, Y.-Y. Huang, R. Yin, L.R. Perussi, G.P. Tegos, J.R. Perussi, T. Dai, M.R. Hamblin, Photodynamic inactivation of biofilm: taking a lightly colored approach to stubborn infection, Expert Rev. Anti. Ther. 11 (2013) 669–693, https://doi.org/10.1586/14787210.2013.811861.

[3] L. Huang, Y. Xuan, Y. Koide, T. Zhiyentayev, M. Tanaka, M.R. Hamblin, Type i and Type II mechanisms of antimicrobial photodynamic therapy: an in vitro study on gram-negative and gram-positive bacteria, Lasers Surg. Med. 44 (2012) 490–499, https://doi.org/10.1002/lsm.22045.

[4] V. Kussovski, V. Mantareva, I. Angelov, P. Orozova, D. Wöhrle, G. Schnurpfeil, E. Borisova, L. Avramov, Photodynamic inactivation of aeromonas hydrophila by cationic phthalocyanines with different hydrophobicity, FEMS Microbiol. Lett. 294 (2009) 133–140, https://doi.org/10.1111/j.1574-6968.2009.01555.x.

[5] T.N. Demidova, M.R. Hamblin, Photodynamic therapy targeted to pathogens, Int. J. Immunopathol. Pharmacol. 17 (2011) 245–254 http://www.ncbi.nlm.nih.gov/pubmed/23190896.

[6] T.N. Demidova, M.R. Hamblin, Effect of cell-photosensitizer binding and cell density on microbial photoinactivation, Antimicrob. Agents Chemother. 49 (2005) 2329–2335, https://doi.org/10.1128/AAC.49.6.2329-2335.2005.

[7] T. Maisch, A new strategy to destroy antibiotic resistant microorganisms: antimicrobial photodynamic treatment, Mini-Rev. Med. Chem. 9 (2009) 974–983, https://doi.org/10.2174/138955709788681582.

[8] T. Maisch, C. Bosl, R.M. Szeimies, N. Lehn, C. Abels, Photodynamic effects of novel XF porphyrin derivatives on prokaryotic and eukaryotic cells, Antimicrob. Agents Chemother. 49 (2005) 1542–1552, https://doi.org/10.1128/AAC.49.4.1542-1552.2005.

[9] J.L.S. Gonçalves, C. Bernal, H. Imasato, J.R. Perussi, Hypericin cytotoxicity in tumor and non-tumor cell lines: a chemometric study, Photodiagn. Photodyn. Ther. 20 (2017) 86–90, https://doi.org/10.1016/j.pdpdt.2017.08.005.

[10] W.C.M.A. Melo, A.N. Lee, J.R. Perussi, M.R. Hamblin, Electroporation enhances antimicrobial photodynamic therapy mediated by the hydrophobic photosensitizer, hypericin, Photodiagn. Photodyn. Ther. 10 (2013) 647–650, https://doi.org/10.1016/j.pdpdt.2013.08.001.

[11] C. Bernal, T.T. Tominaga, A.O. Ribeiro, H. Imasato, J.R. Perussi, Comparative studies of photophysical and biological properties of hypericin and hypericin-glucamine, Photodiagn. Photodyn. Ther. 8 (2011) 190, https://doi.org/10.1016/j.pdpdt.2011.03.226.

[12] C. Bernal, J.A.O. Rodrigues, A.P.P. Guimarães, A.O. Ribeiro, K.T. Oliveira, H. Imasato, J.R. Perussi, Selective photoinactivation of C. albicans and C. dubliniensis with hypericin, Laser Phys. 21 (2010) 245–249, https://doi.org/10.1134/S1054660X1101004X.

[13] A.R. Kamuhabwa, R. Roelandts, P.A. De Witte, Skin photosensitization with topical hypericin in hairless mice, J. Photochem. Photobiol. B Biol. 53 (1999) 110–114, https://doi.org/10.1016/S1011-1344(99)00135-9.

[14] B. Krammer, T. Verwanger, Molecular response to hypericin-induced photodamage, Curr. Med. Chem. 19 (2012) 793–798 http://www.ncbi.nlm.nih.gov/pubmed/22214453.

[15] F.E. Fox, Z. Niu, A. Tobia, A.H. Rook, Photoactivated hypericin is an anti-proliferative agent that induces a high rate of apoptotic death of normal, transformed, and malignant T lymphocytes: implications for the treatment of cutaneous lymphoprohferatlve and inflammatory disorders, J. Invest. Dermatol. 111 (1998) 327–332, https://doi.org/10.1046/j.1523-1747.1998.00278.x.

[16] V. Engelhardt, B. Krammer, K. Plaetzer, Antibacterial photodynamic therapy using water-soluble formulations of hypericin or mTHPC is effective in inactivation of Staphylococcus aureus, Photochem. Photobiol. Sci. 9 (2010) 365–369, https://doi.org/10.1039/b9pp00144a.

[17] C.M.N. Yow, H.M. Tang, E.S.M. Chu, Z. Huang, Hypericin-mediated photodynamic antimicrobial effect on clinically isolated pathogens, Photochem. Photobiol. 88 (2012) 626–632, https://doi.org/10.1111/j.1751-1097.2012.01085.x.

[18] A. Rezusta, P. López-Chicón, M.P. Paz-Cristobal, M. Alemany-Ribes, D. Royo-Díez, M. Agut, C. Semino, S. Nonell, M.J. Revillo, C. Aspiroz, Y. Gilaberte, In vitro fungicidal photodynamic effect of hypericin on Candida species, Photochem. Photobiol. 88 (2012) 613–619, https://doi.org/10.1111/j.1751-1097.2011.01053.x.

[19] J.R. Perussi, Inativação Fotodinâmica de Microrganismos, Química Nova 30 (2007) 988–994, https://doi.org/10.1590/S0100-40422007000400039.

[20] V. Stupáková, L. Varinská, A. Mirossay, M. Sarisský, J. Mojzis, R. Dankovcík, P. Urdzík, A. Ostró, L. Mirossay, Photodynamic effect of hypericin in primary cultures of human umbilical endothelial cells and glioma cell lines, Phytother. Res. 23 (2009) 827–832, https://doi.org/10.1002/ptr.2681.

[21] W.C.M.A. Melo, J.R. Perussi, Comparando inativação fotodinâmica e antimicrobianos, Rev. Ciencias Farm. Basica e Apl. 33 (2012) 331–340.

[22] M.D. Cantley, P.M. Bartold, V. Marino, R.C. Reid, D.P. Fairlie, R.N. Wyszynski, P.S. Zilm, D.R. Haynes, The use of live-animal micro-computed tomography to determine the effect of a novel phospholipase A2 inhibitor on alveolar bone loss in an in vivo mouse model of periodontitis, J. Periodontal Res. Suppl. 44 (2009) 317–322, https://doi.org/10.1111/j.1600-0765.2008.01132.x.

[23] M.L. Bouxsein, S.K. Boyd, B.A. Christiansen, R.E. Guldberg, K.J. Jepsen, R. Mu, Guidelines for assessment of bone microstructure in rodents using micro – computed tomography, J. Bone Miner. Res. 25 (2010) 1468–1486, https://doi.org/10.1002/jbmr.141.

[24] J.B. César-Neto, B.B. Benatti, E.A. Sallum, M.Z. Casati, F.H. Nociti, The influence of cigarette smoke inhalation and its cessation on the tooth-supporting alveolar bone: a histometric study in rats, J. Periodontal Res. Suppl. 41 (2006) 118–123, https://doi.org/10.1111/j.1600-0765.2005.00844.x.

[25] C. Pavone, A. Vilas, B. Nogueira, P.S. Cerri, E.M. Jr, R. Adriana, C. Marcantonio, Treatment of periodontal disease with an Er, Cr : YSGG laser in rats exposed to cigarette smoke inhalation, (2015) 2095–2103. doi:10.1007/s10103-015-1731-8.

[26] P. Zanoli, Role of hyperforin in the pharmacological activities of St. John's Wort, CNS Drug Rev. 10 (2004) 203–218, https://doi.org/10.1111/j.1527-3458.2004.tb00022.x.

[27] B. Martínez-Poveda, A.R. Quesada, M.Á. Medina, Hyperforin, a bio-active compound of St. John's Wort, is a new inhibitor of angiogenesis targeting several key steps of the process, Int. J. Cancer 117 (2005) 775–780, https://doi.org/10.1002/ijc.21246.

[28] U. Wölfle, G. Seelinger, C.M. Schempp, Topical application of St. john´s wort (Hypericum perforatum), Planta Med. 80 (2014) 109–120, https://doi.org/10.1055/s-0033-1351019.

[29] W.C.M.A. Melo, L.F. Castro, R.M.M.T.S. Dalmas, J.R. Perussi, *Effectiveness of photodynamic therapy on Gram-negative bacteria*, Antonio Méndez-Vilas. (Org.). Science Against Microbial Pathogens: Communicating Current Research and Technological Advances 1 Formatex Research Center, Spain, 2011, pp. 662–667.

[30] H. Choi, W. Lim, I. Kim, J. Kim, Y. Ko, H. Kwon, S. Kim, K.M. Kabir, X. Li, O. Kim, Y. Lee, S. Kim, O. Kim, Inflammatory cytokines are suppressed by light-emitting diode irradiation of P.gIngivalis LPS-treated human gingival fibroblasts: inflammatory cytokine changes by LED irradiation, Lasers Med. Sci. 27 (2012) 459–467, https://doi.org/10.1007/s10103-011-0971-5.

[31] P. D'Andrea Fonseca, F.M. De Lima, D.T. Higashi, D.F.V. Koyama, D. De Oliveira Toginho Filho, I.F.L. Dias, S. De Paula Ramos, Effects of light emitting diode (LED) therapy at 940 nm on inflammatory root resorption in rats, Lasers Med. Sci. 28 (2013) 49–55, https://doi.org/10.1007/s10103-012-1061-z.

[32] J. Dai, Y. Ma, M. Shi, Z. Cao, Y. Zhang, Initial Changes in Alveolar Bone Volume for Sham-operated and Ovariectomized Rats in Ligature-induced Experimental Periodontitis, (2016), pp. 581–588, https://doi.org/10.1007/s00784-015-1531-3.

[33] P.M. Duarte, K.R. Tezolin, L.C. Figueiredo, M. Feres, M.F. Bastos, Microbial profile of ligature-induced periodontitis in rats, Arch. Oral Biol. 55 (2010) 142–147, https://doi.org/10.1016/j.archoralbio.2009.10.006.